June 2005

Investigation of Variability of the North Atlantic Subtropical Mode Water Using Profiling Float Data and Numerical Model Output

Ge Peng[1], Eric P. Chassignet[1], Young-Oh Kwon[2], and Stephen C. Riser[3]

[1] Rosenstiel School of Marine and Atmospheric Science
University of Miami, Miami, FL 33149

[2] Climate and Global Dynamics Division, NCAR
Boulder, CO 80305

[3] School of Oceanography, University of Washington
Seattle, WA 98195

Corresponding author:

Dr. Ge Peng, MPO/RSMAS
University of Miami, 4600 Rickenbacker Causeway
Miami, FL 33149, USA. Email: gpeng@rsmas.miami.edu
Phone: (1) 305 - 421 - 4108; Fax: (1) 305 - 421 - 4696

Abstract

The basic characteristics of the North Atlantic Subtropical Mode Waters (STMW) are well documented in the literature from one-time hydrographic sections or from long term measurements at one location. From July 1997 to March 1998, 71 vertical profiling floats were deployed in the Western Subtropical North Atlantic region to provide a broader spatial and temporal coverage of the STMW. In this study, the STMW properties are estimated from a total of 5352 float temperature profiles in an area covering $30^0W - 80^0W$ and $20^0N - 45^0N$, from January 1998 to December 2000. These STMW properties are compared to those derived from numerical simulation output using the Miami Isopycnic-Coordinate Model (MICOM). The model is configured to the North Atlantic Ocean with a 1-degree horizontal resolution and 20 vertical layers. The model temperature profiles are collocated with the observed float profiles for a direct comparison.

The values of the mean STMW temperature derived from both the float data and model output are roughly equal (18.1^0C for floats and 18.0^0C for the model). The model is found to capture well the observed annual cycle of the STMW volume. Given good agreement between float and model profiles, we use a longer MICOM simulation to investigate decadal variability of the STMW renewal rate in terms of the annual subduction rate and its relationship to the large-scale atmospheric circulation pattern changes measured by the North Atlantic Oscillation index. Good correlation is found between the model annual subduction rate anomaly at the Panulirus Station and the NAO winter index anomaly on decadal time scales with NAO leading by 2 - 3 years.

1. Introduction

The North Atlantic Subtropical Mode Waters (STMW hereafter) are the water masses found between the seasonal and permanent thermoclines in the northwestern and central portions of the subtropical gyre in the western North Atlantic ocean. The basic characteristics of STMW are well documented in the literature. The temperature of STMW is about 18^0C, i.e., the 18-degree water has been used to characterize this water mass. The STMW layer has been observed to ventilate to depths as great as 900 m, with a mean penetration of about 287 m and a mean thickness of about 200 m (Worthington, 1959; Talley and Raymer, 1982; Joyce and Robbins, 1996; Talley, 1996; Joyce et al., 2000). STMW is believed to be bounded by the Gulf Stream to the northwest, 19^0N to the south, and approximately 45^0W to the east (Worthington, 1959; Istoshin, 1961). New water is produced at the end of each winter through convection driven by intense wintertime buoyancy loss (McCartney, 1982). The winter vertical convection takes place in the so-called "subduction zone" (New et al., 1995) where sloping isopycnals outcrop at the surface in the Sargasso Sea. Although Ekman pumping has traditionally been viewed as a primary mechanism for transferring surface waters into the thermocline, studies in the last two decades have established that the newly formed STMW is largely subducted or drawn downward through the spatially and temporally varying base of the mixed layer into the ocean interior along the sloping isopycnals. The amount of water mass that enters the permanent thermocline is determined by the annual subduction rate, which therefore affects the properties of STMW and the renewal rate. It is not clear whether, and not likely, that all the STMW is renewed each year. The fraction of

STMW renewed, or the STMW renewal rate, is estimated to be in a range of 20% to 25% per year (Worthington, 1959; Jenkins, 1982).

Continuous records of STMW are rare. STMW-related studies have largely relied on one-time hydrographic sections or long term measurements at one location. The longest point measurements to date are the hydrographic time series at the Panulirus Station (64.5^0W, 32.2^0N, Bermuda), which is located in the westward return flow of the subtropical gyre. This dataset provides one of the few records for examining temporal variability and has been used by most of the previous observational studies related to STMW. Properties of STMW at the Panulirus Station showed interannual variations and slight property shifts before and after 1972 (Talley and Raymer, 1982). The potential temperature and salinity were 18^0C and 36.5 (PSS-78) from 1954 to 1971 but 17.1^0C and 36.4 from 1972 to 1975; thus the STMW was cooler and fresher in the latter period, indicating temporal variability that was later suggested to be driven by variability in the wintertime cooling of the Gulf Stream region (Marsh and New, 1996). Using World Ocean Atlas 1994 data, which covers the period from 1968 to 1988, Alfultis and Cornillon (2001) showed that spatial variations existed in distributions of the STMW properties even on a 2.5^0 latitude $\times$ 5.0^0 longitude grid.

Since July 1997, 71 PALACE profiling floats were launched in the western North Atlantic as part of the World Ocean Circulation Experiment (WOCE)/Atlantic Circulation and Climate Experiments (ACCE), designed to examine the climatology of North Atlantic STMW. Unlike research cruise measurements that only yield continuous measurements for short pe-

riods of time, floats collect vertical profiles continuously over their lifetime. In contrast to point measurements such as the one at the Panulirus Station, floats also provide a broad spatial coverage in addition to high temporal sampling. Such coverage provides an opportunity to validate the performance of ocean numerical models in simulating STMW. In this paper, we first evaluate the ability of the Miami Isopycnic Coordinate Ocean Model (MICOM) to simulate the STMW properties using the float data in an area covering $30^0W - 80^0W$ and $20^0N - 45^0N$, from January 1998 to December 2000. The model consists of 19 interior isopycnic layers and a spatially and temporally varying mixed layer. This choice of vertical coordinate and model configuration has a better representation of seasonally varying water property front and clearer separation of isopycnal and diapycnal mixing. Therefore, it provides a natural framework for handling the formation and ventilation processes of STMW, mainly due to but not limited to the following reasons: the STMW mass forms within a selected density range; the newly formed surface STMW is primarily subducted through the spatially and temporally varying base of the mixed layer into the ocean interior along the sloping isopycnals; a majority of transport occurs along isopycnal surfaces; and isopycnal mixing is predominant (Jenkins, 1982; Bleck and Chassignet, 1994; New et al., 1995; Paiva and Chassignet, 2002). Previous work has shown that MICOM is capable of capturing the decadal variability of the STMW potential vorticity (PV) anomaly (Paiva and Chassignet, 2002), which is intimately tied with the STMW layer thickness. The result from this paper will show in section 4 that the model captures well the annual cycle of observed STMW volume. The good agreement that exists between the model and observations then enables

us to examine the long-term variability of the STMW renewal rate in terms of the annual subduction rate and its response to atmospheric forcing variability, such as that associated with the North Atlantic Oscillation (NAO), using model output from simulations spanning the period of 1946 - 2000 (55 years).

The paper is organized as follows. The observational data and the model configuration used in this study are outlined in section 2. Comparison of float data and model output is shown in section 3. The estimates of STMW properties will be shown in section 4 along with their variability in both float-derived and model-derived STMW properties. The variability of the model annual subduction rate and its correlation with the winter NAO index will be examined in section 5. A summary of the results is given in section 6.

2. Data and model configuration

2.1. Profiling float data

The observational data for this study are the vertical temperature profiles collected by profiling floats deployed in the western subtropical North Atlantic region. Between July 1997 and March 1998, 71 PALACE profiling floats were deployed in that region to collect temperature profiles in the upper 1000 m at about 10-day intervals. The floats were programmed to drift at a nominal depth of 1000 m (parking depth) for about 10 days, and the measurements were made as the floats ascended to the sea surface from the parking depth at the end of each cycle (Roemmich et al., 2004). Temperature measurements were taken at approximately 100 depths between 1000 m and the sea surface during the ascents. The vertical interval for the float profiles, therefore, ranges from 5 m to 20 m. The accuracy of temperature measured

by the floats was estimated to be 0.01^0C over several years during the deployment phase (Roemmich et al., 2004). A total of 5352 temperature profiles collected from January 1998 to December 2000 are used in this study. The profiles are grouped monthly. The number of profiles ranges from 81 to 180 per month, averaging 150 per month (Fig. 1a). The float deployment locations for all 71 floats and their trajectories after deployment are shown in Fig. 1b. Figs. 2a,b display the geographic locations of the profiles for the months of January 1998 and March 1999, representing the worst and best cases in terms of the number of profiles within the region, respectively. (The dashed lines represent the profiling sampling coverage area.) Both cases show that a fairly good spatial coverage of the Sargasso Sea is obtained despite the uneven sampling. Float data coverage, however, is sparse east of the mid-Atlantic Ridge region as well as in the Canary Basin.

The float data coverage varies monthly (see Fig. 2c for the outlines of the monthly float data sampling area). To eliminate the possible impact of an unsteady sampling area, STMW properties are computed in a "common domain", the area outlined by the thick dashed line in Fig. 2c, which remains by definition unchanged throughout the study period.

2.2. Model configuration

The ocean numerical model is the Miami Isopycnic Coordinate Ocean Model (Bleck et al. 1992; Bleck and Chassignet 1994). The model is configured for the North and Equatorial Atlantic Ocean Basin from 28^0S to 70^0N with realistic topography derived from the $1/12^0$ ETOPO5 data set (Fig. 3). The horizontal grid is defined on a Mercator projection, with a 1^0 grid interval in longitude and $1^0 \times cos\phi$ in latitude. The northern and southern lateral

boundaries are closed with buffer zones. The southern buffer zone is about 3^0 wide as in the previous study of Paiva and Chassignet (2002), but the northern boundary has been moved to 70^0N from 65^0N and boundary treatment is similar to that in DYNAMO (DYNAMO, 1997) (see Fig. 3 for details). The salinity and layer interface depths in the buffer zones are restored toward monthly Levitus climatology (Levitus, 1982). The Mediterranean Sea is not included in the model domain. The outflow of salty Mediterranean water into the Atlantic is represented by relaxing salinity to Levitus climatology in a buffer zone placed at the Gulf of Cádiz. There are 20 layers in the vertical with a thermodynamically active Kraus-Turner surface mixed layer. The σ_θ values for the nineteen interior layers are 24.70, 25.28, 25.77, 26.18, 26.52, 26.80, 27.03, 27.22, 27.38, 27.52, 27.64, 27.74, 27.82, 27.88, 27.92, 28.00, 28.06, 28.09, and 28.12. For other model details, the reader is referred to Paiva and Chassignet (2002).

Compared to float data point distributions, the model grid points are on a regular grid and the horizontal coverage is greater on average than that given by the float data. Locally, the float data can provide higher spatial resolution (Fig. 2d). The float profiles, on average, also have higher vertical resolution than the corresponding profiles derived from the model.

The model is initialized from the January state of Levitus (1982) and spun up for 20 years with the European Centre for Medium-Range Weather Forecasts (ECMWF) monthly climatological atmospheric forcing. The model is then integrated for additional 22 years with monthly atmospheric forcing derived from 6-hourly ECMWF fields from 1979 to 2000.

In the work of Paiva and Chassignet (2002), the model was forced with atmospheric data

from 1946 to 1989 derived from the Comprehensive Ocean-Atmosphere Data Set (COADS) (Da Silva et al., 1994) and demonstrated the ability to capture the decadal variability of STMW PV anomaly at the Panulirus Station. In this paper, we will first focus on the period from January 1998 to December 2000, comparing the model profiles to the float profiles to determine if the model is capable of capturing the STMW water and to examine the variability of STMW over the common domain with both float data and model output. The model output from the entire integration period from year 1979 to 2000 will be used, along with the 1946-89 simulation, when exploring the variability of the model-based annual subduction rate at longer temporal scales in Section 6.

3. Comparison of float data and model output

Since observed float profiles are not evenly distributed in space, monthly composite profiles are created by binning the individual profiles in 1^0 boxes. An objective analysis (OA) scheme (Bretherton et al. 1976) is then applied to interpolate the binned float profiles onto a 1^0 regular grid in the area covering $30^0W - 80^0W$ and $20^0N - 45^0N$, before the float-based STMW properties are computed.

Model output is subsampled by interpolating model profiles onto the float locations. The above procedure used for the float observations is then applied to the interpolated model profiles when computing the model-based STMW properties. Tests of the OA scheme with native grid model output show that the OA procedure reproduces well the horizontal distribution of model variables within the spatial coverage of the float sampling area. The largest errors in the OA procedure are found mainly outside the data coverage region (north of

the Gulf Stream and the southeast corner of the STMW region). Since only profiles within the common domain are used in calculating the STMW properties using float or model profiles, the impact of the OA procedure on the estimated STMW properties is minimal.

Two examples of float and model temperature profiles selected randomly at locations near the Panulirus Station are shown in Fig. 4. The float profiles are represented by thin solid lines. The step-like solid lines are for the original isopycnic model profiles, and the dashed lines are for the vertically interpolated model profiles. If STMW is defined as water masses between 17 and 19^0C, we can see that, for these two examples, the model profile in October 1998 compares well with the float profile, while the model profile in August 1998 would induce a STMW layer that is located at greater depth than the corresponding float profile. Overall, these two model profiles appear to capture reasonably well the basic features of STMW such as temperature and layer thickness, when compared to those from floats.

Based on historical observations, the mean observed STMW salinity value for the Panulirus Station ranges from 36.40 to 36.60 (Worthington, 1959; Talley and Raymer, 1982; Joyce and Robbins, 1996; Talley, 1996). In the model, the mean STMW salinity for the period from year 1998 to 2000 is 36.45 which is on the low end of the observed salinity but within the general STMW salinity range. The mean salinity profile, however, compares well in the upper 500 m to that of Joyce and Robbins (1996) (Fig. 5).

Fig. 6 shows meridional cross-sections of temperature along the 53^0W and 64^0W sections. Tracing the areas bounded by the 17^0C and 19^0C isolines (thick solid lines represent model profiles and thick dashed lines float profiles), it is seen that the depth of the model-derived

STMW layer is generally between 200 m and 400 m, fairly consistent with the observations. In winter, there is a well-mixed layer between 17^0C and 19^0C that extends from the ocean surface to over 400 m and allows the 18-degree water to be subducted into the interior ocean layers. This is not the case during the summer months, and the seasonal changes are minimal south of 30^0N in both sections. Most of the observed STMW is located south of 37^0N, while in the model it extends farther north, reflecting the fact that the modeled Gulf Stream overshoots Cape Hatteras (Chassignet et al., 2003).

4. Estimated STMW temperature and volume

The STMW temperature and volume are computed in the common domain using the criteria of a temperature range of 17 - 19 ^0C and a vertical temperature gradient of less than 0.01 $^0C/m$. (The sensitivity of STMW temperature and volume to the choice of vertical temperature gradients using the float data is given in Appendix A).

The values of the mean STMW temperature derived from the float and model profiles are roughly equal (18.1 ± 0.24^0C for floats and 18.0 ± 0.17^0C for the model.) The model-derived STMW layer thickness is $\sim$ 245 m, which is larger than in the observations ($\sim$ 190 m). This large value in the model-derived STMW layer thickness is mostly due to the fact that the path of the modeled Gulf Stream is farther north than observed and the STMW layer base extends quite deep in this region (see Fig. 6 for detail and discussion in section 3.) The corresponding value of model-derived STMW volume is also larger ($\sim 7 \times 10^5$ km^3), when compared to that of float-derived ($\sim 6 \times 10^5$ km^3). The remainder of this section describes, in both observations and the model, spatial distributions of annual mean STMW temperature,

layer thickness, and depth of the STMW layer, as well as the temporal evolution of spatially averaged STMW temperature and volume.

4.1. Spatial distributions of time mean

There is a well defined warm core in both float- and model-based time mean STMW temperature distributions (Fig. 7a,b). The core of the float-derived STMW temperature is elongated southwest-northeast with a strong gradient, while the model-derived core is elongated almost north-south with a much weaker gradient (Fig. 7a,b). The float- and model-based STMW layer thickness fields show that the most of the STMW is captured by the common domain area with the model STMW shifted farther north (Fig. 7c,d). The float-based STMW layer lies deeper near the northwestern portion of the subtropical gyre, with upper depth of the STMW layer beginning near the surface in the northeast half of the domain and dropping from 150 m at 52^0W to just over 250 m toward the west at 62^0W (Fig. 7e). The upper depth of the model-based STMW layer begins near the surface in the northeast half of the domain as well, but drops steeply from about 100 m at 55^0W to 325 m at 65^0W, slightly west and with stronger drop-off rate than seen in the observations (Fig. 7f). In summary, the major difference between the distributions of the model- and float-based STMW properties is found in the northern edge of the common domain between 50^0W - 65^0W, mainly as a result of the Gulf Stream system being located farther north in the model than in observations. Additionally, since eddies act to diffuse STMW properties in the region, the fact that the model is not eddy-resolving and the effect of eddy diffusion in the model is parameterized with a constant thickness diffusion velocity of 0.5 cms^{-1}, may

also contribute to the differences between the distributions of the model- and float-based STMW properties as the effect of eddies is highly inhomogeneous in the real world.

4.2. Temporal evolution of spatial mean

Considering both the float- and model-based estimates, the spatially averaged STMW temperature is observed to vary (over the 1998-2000 period) between 17.9 and 18.3^0C (Fig. 8a), a range of STMW temperature that is consistent with previous studies (Worthington, 1959; Joyce et al., 2000). The temporal variability in float-based estimates of spatially-averaged STMW temperature may be explained by a variety of factors such as: interannual-to-decadal variability in the large-scale atmospheric forcing; sampling of high frequency (synoptic) variability in the forcing; sampling of mesoscale variability due to eddies; and the residual "memory" of past variability, such that the STMW temperature corresponds to a mixture of newly-formed STMW and the STMW formed in previous years. No pronounced annual cycle of STMW temperature has been observed as the temperature of newly formed surface mode water tends to be in the same range as that of previously formed subsurface mode water. STMW temperature is actually more dominated by interannual-decadal variability as shown by localized observations (Talley and Raymer, 1982; Klein and Hogg, 1996). However, the STMW temperature can be modified by high frequency forcing and eddies and the stochastic nature of the latter makes it difficult to properly hindcast the short-term STMW temperature variability. This is even more difficult when using a non-eddy resolving model forced without synoptic variability. Previous work has shown that MICOM is capable of capturing the decadal variability of the mode waters (Paiva and Chassignet,

2002), but the time series for the comparison between float and model data, being only three years long, is too short to discuss the interannual-decadal variability. As one would expect, the agreement is poor in the month-to-month variability of STMW temperature between the float and the model and no significant correlation is observed between them (Fig. 8b,c).

The power spectral density function, on one hand, shows intra-annual, and seasonal peaks for the float data. The model time series, on the other hand, exhibits no annual peak, but has a more pronounced seasonal signal than the float data (Fig. 8d). These STMW temperature variations are associated with the renewal of STMW as a result of subduction and the evolution of the seasonal thermocline. The annual peak in the power spectral density function estimates of time series of the float temperature may not be significant due to the limited record length[1].

In contrast to the temperature series, both spatially averaged STMW volume time series show distinct annual and semiannual cycles with a maximum correlation of 0.74, with the model leading floats by approximately one month (Fig. 9). The annual cycle peaks in the spring (March to May) and are associated with the production of new STMW. The one-month time lag in the model in relation to the float data can be clearly seen in the years 1999 and 2000, but not in 1998. This indicates that this lag is not representative of a systematic bias in the model. The model may, however, respond more slowly than the observations to changes in atmospheric forcing associated with the transition from a negative to positive NAO index in the 1998-2000 years (Fig. 12). Overall, with new mode water forming each

[1]Spectral estimates of periods of one year or more are not necessarily accurate with records spanning only a few years.

winter and being depleted each fall, the STMW volume goes through a distinct annual cycle. Although the values of the observed and modeled STMW volume differ, the model is able to capture the annual cycle and the modeled time series is highly correlated with the observations.

5. The annual subduction rate and its correlation with NAO

The formation of new STMW is associated with the subduction of the 18-degree water, vertically homogenized through deep convection driven by wintertime buoyancy loss (McCartney, 1982). As the detrainment process takes the surface and mixed layer water mass into the ocean interior through the base of the mixed layer, only a fraction of the detrained water finds its way to the permanent pycnocline and becomes new STMW water (Qiu and Huang, 1995). The annual subduction rate defines the water mass that enters the permanent pycnocline through the base of the mixed layer via the seasonal pycnocline in the subtropics (Marshall et al., 1993; Qiu and Huang, 1995). Therefore, variability of the STMW renewal rate can be quantified by the variability of the annual subduction rate. To investigate this variability, the annual subduction rate is computed and examined using model results in this section. The spatial distribution of the annual subduction rate for the years 1998 to 2000 is first described in section 5.1, to examine spatial variability and differences between years. Then, in section 5.2, the decadal variability of the annual subduction rate and its correlation with the winter NAO index will be explored using model output from 1946 to 2000.

5.1. Spatial and temporal distributions of the annual subduction rate

Following the definition and method of computing the annual subduction rate described in Marshall et al. (1993) and Marsh and New (1996), the annual subduction rate, S_{ann}, is expressed as follows,

$$S_{ann} = -\overline{w_{EK}} + \frac{\beta}{f}\int_{-H}^{0} \overline{v} dz - \overline{\mathbf{u_H}} \cdot \nabla H \tag{1}$$

where w_{EK} is the Ekman pumping velocity, v is the meridional velocity component of the horizontal velocity, $\mathbf{u}$. f is the Coriolis parameter and β is its meridional gradient. H is the maximum depth of the winter mixed layer. An overbar denotes an annual average and the subscript H indicates that the quantity is evaluated at the depth H.

In this expression, the first two terms on the right hand side represent the volume flux due to downward vertical pumping which is related to the Ekman pumping and the meridional transport within the mixed layer. The third term is the lateral induction term, which computes the amount of water that is carried away horizontally through the sloping mixed layer base.

The model annual subduction rates for years 1998 to 2000 are shown in Fig. 10a-c. The three year mean is shown in Fig. 10d. In agreement with horizontal distributions shown in Marshall et al. (1993) and Marsh and New (1996), the distributions of the annual subduction rate for all three years and for the three-year-mean show a band of high subduction rate extending across the subtropical gyre with multiple centers. In this subduction zone, the newly formed surface STMW water was mainly drawn downward into the ocean interior along

sloping isopycnals through the base of the wintertime mixed layer, by lateral induction. The annual subduction rate can be enhanced by Ekman pumping and reduced by the meridional transport within the mixed layer. It is the fluid that enters the permanent thermocline through the lateral induction process that actually ventilates the thermocline (Marshall et al., 1993). Despite the fact that the modeled Gulf Stream is located farther north than observed, the model annual subduction rates are in excellent agreement with the climatological estimate of Marshall et al. (1993). Both analyses put the zero line of S_{ann} at approximately the zero Ekman pumping line separating the two gyres. Since the main term contributing to S_{ann} is the lateral induction rate, $-\overline{\mathbf{u_H}} \cdot \nabla H$, one could have expected a northward displacement of the zero line in response to a northward displacement of the mixed layer shoaling at the Gulf Stream's southern edge associated with the Gulf Stream's northward displacement. However, the modeled Gulf Stream is also much broader than observed and the location of the mixed layer shoaling at its southern edge remains close to the climatological data used by Marshall et al. (1993). Thus, the impact of the position of the modeled Gulf Stream on the downward annual subduction rate is minimal.

The STMW renewal rate can be calculated by dividing the annual STMW formation (or production) rate by the average volume with the production rate being the area-integrated annual subduction rate within the STMW formation region. The STMW formation region can be loosely defined by the region where the March mixed layer temperature ranges between 17^0C and 19^0C. The mean model STMW renewal rate is about 24% per year, which is consistent with the STMW renewal rate estimated by Worthington (1959) and

Jenkins (1982).

The spatial distribution of the annual subduction rate does not vary greatly from one year to another, although slight displacements do occur. The Panulirus Station, which is a reference site for STMW studies with the longest running observational record so far, is often located at the boundary between the negative (obduction) and positive (subduction) annual subduction rate regime (filled circle in Fig. 10 denotes the location of the Panulirus Station). It is located within the subduction region for the year 1998 and 1999 but only falls within the STMW formation region for the year 1998. Monthly time evolution of the model temperature profiles indicates that the 19^0C isotherm only outcrops at the surface in the winter of 1998 but not in the winters of 1999 and 2000 (Fig. 11a). Thus, the 18-degree water is rarely formed at this location, largely because the surface temperature is too high to be considered as the 18-degree water. It can, however, form at this location if the surface temperature has been cooled down enough, for example, in the winter of 1998. Both float and model temperature profiles near or at the Panulirus Station have displayed a distinct vertically homogeneous layer extending all the way to the surface with a mean layer temperature of about 18.9 and 18.8^0C, respectively (Fig. 11b). The values of the mean STMW temperature for the entire STMW layer (both new and old STMW) are 18.4^0C for the float profile and 18.6^0C for the model. As the sea surface temperature is influenced by the large-scale atmospheric circulation changes and air-sea heat flux (Cayan, 1992a; Cayan, 1992b), STMW formation and STMW properties at this location are particularly sensitive to atmospheric forcing changes. The STMW properties such as temperature and potential

vorticity at this location has been shown to exhibit decadal variability (Joyce and Robbins, 1996), which has been found to be correlated with NAO index (Talley and Raymer, 1982; Joyce et al., 2000; Paiva and Chassignet, 2002; Kwon and Riser, 2004). Whether or not the 18-degree water is formed locally or formed elsewhere and subsequently transferred to this location in the mixed layer, it is through the subduction process that the 18-degree water is transported irreversibly into the permanent pycnocline. The long-term accumulation of above (below) normal subduction rate will transfer more (less) than normal STMW mass into the permanent pycnocline, and therefore, increase (reduce) STMW layer thickness and decrease (increase) STMW PV. Of course, the subduction process is not the only process that may alter the STMW properties. Horizontal advection and lateral mixing of STMW properties can also contribute to a certain degree in altering the STMW properties. However, in this study, we will focus on whether there is long-term variability in the annual subduction rate, which measures the amount of the mode water being transported irreversibly to the permanent pycnocline, and whether the subduction rate is correlated to NAO, which is associated with the large-scale atmospheric forcing changes, using the time series of the model annual subduction rate that extends from 1946 to 2000.

5.2. Decadal variability of the annual subduction rate and its correlation to NAO

a) At the Panulirus Station

The time series of the annual subduction rate anomaly at the Panulirus station is constructed from the model run that is forced by the 1979-2000 ECMWF atmospheric forcing as described in section 2. Since the 1979 to 2000 period is biased toward high NAO years,

the time series was extended to 1946 by combining the subduction rate from a second model run forced by COADS (Da Silva et al., 1994) from 1946 to 1989. This gives a total of 55 years from 1946 to 2000 with 11 years overlapping (1979-1989). During the overlap, the two time series of the annual subduction rate were found to be fairly consistent with one another and a simple averaging was used to merge the series.

To show the integral effect of the annual subduction rate anomaly, the annual subduction rate anomaly is integrated in time for the duration of the model output. The time evolution of this integrated annual subduction rate anomaly at the Panulirus Station is shown in Fig. 12a. Decadal variability of the integrated annual subduction rate from the combined time series is very distinct. A broad range of significant correlation coefficients are found between the integrated annual subduction rate anomaly and the winter NAO index anomaly (Fig. 12b). The cross correlation between the two low-pass filtered time series shows a peak that is corresponding to the NAO index leading the annual subduction rate by 2 - 3 years (Fig. 12d). This is consistent with the work of Paiva and Chassignet (2002) who indicated that, at near-decadal time scales, the variability in STMW formation in terms of PV anomaly can be largely attributed to the variability of the integrated surface heat flux that may be generated through changes in the large-scale atmospheric circulation with the STMW PV anomaly lagging NAO by 2 - 3 years. The variations of the STMW formation may not be tied closely to those of the surface heat flux on an individual year basis (Talley and Raymer, 1982; Paiva and Chassignet, 2002), but the low-frequency variability of the surface heat flux at the Panulirus Station is found to be correlated with that of the NAO with zero-lag

(Fig. 13).

b) Over the STMW formation region

Although the Panulirus Station is a well studied site due to its long-lasting hydrographic record, it is also necessary to know if the decadal variability displayed at the Panulirus Station is representative for the entire STMW formation region. We define the STMW formation region by the region where the March mixed layer temperature ranges between 17^0C and 19^0C (shown by the dashed lines in Fig. 10). The integrated annual subduction rate anomaly time series is constructed as in Section 5.2a using the subduction rate over the STMW formation region (Fig. 14a). Same as for the Panulirus Station, there is a broad range of significant correlation coefficients between the integrated annual subduction rate anomaly and the winter NAO index anomaly (Fig. 14b). The shape of the correlation coefficient function distribution is more symmetric compared to that of the Panulirus Station. The distribution mimics a Gaussian or "Normal" distribution with zero-crossings at lags of -13.5 and 14 years. The cross correlation between the two low-pass filtered time series shows that the NAO index leads the subduction rate by about 0 - 1 year (Fig. 14d). This differs somewhat from that of the Panulirus Station, where the NAO index leads the subduction rate by about 2 - 3 years.

6. Summary

The STMW properties were computed using profiling float observations and numerical model simulation output in the area covering $30^0W - 80^0W$ and $20^0N - 45^0N$, from January

1998 to December 2000. The values of the mean float- and model-based STMW temperature are 18.1 ^{0}C and 18.0^{0}C, respectively. The mean STMW layer thickness is $\sim$190 m for floats and $\sim$245 m for the model, which is larger than for the floats and leads to a larger mean STMW volume. Overall, the model did a reasonable job of capturing the subtropical mode water, simulating the mean STMW temperature, and reproducing the annual and semiannual cycles of the STMW volume.

The reasonable agreement between the model and float data encourages us to construct time series of the annual subduction rate, using model output from simulations spanning the period 1946 - 2000 (55 years), to examine the decadal variability of the STMW renewal rate in terms of the annual subduction rate and its correlation to the large-scale atmospheric circulation changes measured by the winter NAO index. Good correlation is found between the model integrated annual subduction rate anomaly at the Panulirus Station and the winter NAO index anomaly on decadal time scales, with the annual subduction rate lagging the NAO by about 2 - 3 years. This implies the modeled oceanic response to the atmospheric forcing anomalies lagging the NAO by about 2 - 3 years, consistent with the work of Paiva and Chassignet (2002) and Kwon and Riser (2004) based on model results and observations, respectively. A more symmetric correlation function is found between the time series of the subduction rate anomaly for the STMW formation region and the NAO index anomaly. Their cross correlation function distribution mimics a Gaussian distribution with the zero-crossings at lags of -13.5 years and 14 years, with the NAO index leading the subduction rate by about 0 - 1 year.

The results shown here is encouraging for the model, especially considering that the model configuration is non-eddy resolving and is forced without synoptic forcing. However, some differences between model- and float-derived properties, particularly in spatial distribution, do exist. Improvements in model simulations may reduce those discrepancies between model results and observations. For example, a better representation of the Gulf Stream and eddies can be achieved with higher horizontal model resolution (Chassignet and Garraffo, 2001), which should in turn improve the modeled STMW properties. An interannual run at higher resolution ($\sim 1/12^0$) should soon become available.

Since year 2000, fifty ARGO floats (Roemmich et al., 2004) have also been launched in our study region, 2004). Over a 5-year period, the ARGO project will provide approximately twice as many as float profiles as we have used here. The approach used in this study can also be applied to the ARGO data. The combination of the float data from both the ACCE project and ARGO project with high resolution numerical simulation will allow the study of interannual-decadal variability of STMW and the impact of NAO on STMW properties, in addition to providing a better three-dimensional picture of STMW in the north Atlantic. Even with a non-eddy resolving model, our study has shown the merits of extending the comparison past year 2000 and presenting a possibility of monitoring STMW structure and variability in near-operational mode by combing the float data and model simulations forced by operational reanalysis data.

Acknowledgments

Support from the National Science Foundation under Grants OCE 0000042 and and

OCE-9911247 is appreciated. Ge Peng thanks Joe Metzger for help in processing the 6-hourly ECMWF forcing fields, Bob Marsh for help in computing the annual subduction rate, Claes Rooth, Adrian New, and Bill Johns for helpful discussions on subduction of STMW and ventilation of the subtropical gyre, and Linda Smith for her careful editing of the manuscript. In-depth comments and suggestions from two reviewers have improved the clarity of the paper.

Appendix A: Sensitivity of vertical temperature gradient in defining STMW

The definition of STMW is somewhat arbitrary and not unique. It is especially demanding to define STMW over a broad spatial region and time space. Seasonal variations of temperature profiles, particularly the seasonal thermocline, add to the difficulty of defining STMW. The estimates of STMW properties are sensitive to the choices made in the criteria used to define STMW, especially the STMW layer thickness and hence STMW volume. The sensitivity of estimated STMW temperature and volume to the vertical temperature gradient criteria used to define STMW is examined in this Appendix using the observed float data.

The observed temperature gradient for old North Atlantic STMW ranges from 0.005 to 0.009 $^0C/m$, although the newly formed STMW can be nearly homogeneous or have a small temperature gradient ranging from 0.0003 to 0.0008 $^0C/m$ (Worthington, 1977; McCartney et al., 1980; Klein and Hogg, 1996). The sensitivity in estimates of STMW was evaluated for four vertical temperature gradient choices in the 17-19^0C range. These gradients are (1) less than 0.006 $^0C/m$ (0.006dT case), (2) less than 0.010 $^0C/m$ (0.010dT case), (3) less than 0.025 $^0C/m$ (0.025dT case), and no limit (no-dT case)and correspond to the following criteria: strict, general, relaxed, and no-gradient (i.e., all of the 17-19^0C range), respectively.

Fig. 15 shows time series of STMW temperature and volume derived from the float data with the different vertical temperature gradients. The time series of STMW temperature for the 0.010dT case retains the most of seasonal and interannual variations compared to the 0.006dT case but with much less fluctuation. For the STMW volume, variations for all four cases are similar except the amount of STMW water differs. The differences are not

noticeable between the 0.025dT and the no-dT cases.

On one hand, with a strict vertical temperature gradient, some of old mode water may end up being eliminated due to the higher vertical gradient and there is therefore the possibility that variations in spatial and temporal evolution of STMW properties may not be entirely due to changes in physical forcing changes and may be in part associated with the elimination of old STMW mass. On the other hand, with a relaxed or no vertical gradient, water masses that are not well mixed are likely to be included as mode water. Therefore, a good compromise seems to be the vertical temperature gradient of less than 0.01 $^0C/m$.

References

Alfultis, M. A. and P. Cornillon, 2001: A characterization of the North Atlantic STMW layer climatology using World Ocean Atlas 1994 data, *J. Atmos. Oceanic Technol.,* **18**, 2021 – 2037.

Bleck, R., C. Rooth, D. Hu, and L. T. Smith, 1992: Salinity-driven thermocline transients in a wind- and thermohaline-forced isopycnic coordinated model of the North Atlantic. *J. Phys. Oceanogr.,* **22**, 1486 – 1505.

Bleck, R. and E. P. Chassignet, 1994: Simulating the oceanic circulation with isopycnic - coordinate models. In S. K. Majundar, E. W. Mill, G. S. Forbes, R. E. Schmalz, and A. A. Panah (Eds.), *The Oceans: Physical-chemical Dynamics and Human Impact*, pp. 17 – 39. The Pennsylvania Academy of Science.

Bretherton, F. P., R. E. Davis, and C. B. Fandry, 1976: A technique for objective analysis and design of oceanographic experiments applied to MODE-73. *Deep-Sea Res.,* **23**, 559 – 582.

Cayan, D. R., 1992a: Latent and sensible heat flux anomalies over the northern oceans: driving the sea surface temperature. *J. Phys. Oceanogr.,* **22**, 859 – 881.

Cayan, D. R., 1992b: Latent and sensible heat flux anomalies over the northern oceans: The connection to monthly atmospheric circulation. *J. Climate,* **5**, 354 – 369.

Chassignet, E. P., and Z. D. Garraffo, 2001: Viscosity parameterization and the Gulf Stream separation, In "*From Stirring to Mixing in a Stratified Ocean*". Proceedings 'Aha

Huliko' a Hawaiian Winter Workshop. University of Hawaii, January 15 - 19, 2001. P. Muller and D. Henderson, Eds, 37 - 41.

Chassignet, E. P., L. T. Smith, G. R. Halliwell, and R. Bleck, 2003: North Atlantic simulation with the HYbrid Coordinate Ocean Model (HYCOM): Impact of the vertical coordinate choice, reference density, and thermobaricity. *J. Phys. Oceanogr.,* **33**, 2504 – 2526.

Da Silva, A. M., C. C. Young, and S. Levitus, 1994: Atlas of surface marine data 1994. Vol. 1: Algorithms and procedures. NOAA Atlas NES DIS 6, U.S. DoC, NOAA, NESDIS, 83 pp.

DYNAMO group, 1997: Dynamics of North Atlantic models: Simulation and assimilation with high resolution models. Report Nr. 294, Institut für Meereskunde, Germany.

Istoshin, Y., 1961: Formative area of 'eighteen-degree' water in the Sargasso Sea. *Deep-Sea Res.,* **9**, 384 – 390.

Jenkins, W. J., 1982: On the climate of a subtropical ocean gyre: Decade timescale variation in water mass renewal in the Sargasso Sea, *J. Marine Res.,* **40**, Suppl., 265 – 290.

Joyce, T. M., and P. E. Robbins, 1996: The long-term hydrographic record at Bermuda. *J. Climate,* **9**, 3121 – 313.

Joyce, T. M., C. Deser, and M. A. Spall, 2000: The relation between decadal variability of subtropical mode water and the North Atlantic Oscillation. *J. Climate,* **13**, 2550 – 2569.

Klein, B., and N. Hogg, 1996: On the interannual variability of 18 Degree Water formation as observed from moored instruments at 55^0W. *Deep-Sea Res.,* **43**, 1777 – 1806.

Kwon, Y. and S. C. Riser, 2004: Variability of subtropical mode water in the North Atlantic: A history of ocean-atmosphere interaction 1961 - 2000. *Geophys. Res. Lett.,* **31**, L19307, doi:10.1029/2004GL021116.

Levitus, S., 1982: Climatological atlas of the world ocean. *NOAA Prof. Paper. No. 13*, U.S. Govt. Printing Office, 173 pp.

Marsh, R. and A. L. New, 1996. Modeling 18^0 water variability. *J. Phys. Oceanogr.,* **26**, 1059 – 1080.

Marshall, J. C., A. J. G. Nurser, and R. G. Williams, 1993: Inferring the subduction rate and period over the North Atlantic. *J. Phys. Oceanogr.,* **23**, 1315 – 1329.

McCartney, M. S., 1982: The subtropical recirculation of mode waters. *J. Mar. Res,* **40 (Suppl.)**, 427 – 464.

McCartney, M. S., L. V. Worthington, and M. Raymer, 1980: Anomalous water mass distributions at 55^0W in the North Atlantic in 1977. *J. Mar. Res.,* **38**, 147 – 172.

New, A. L., R. Bleck, Y. Jia, R. Marsh, M, Huddleston, and S. Barnard, 1995. An isopycnic model study of the North Atlantic. Part I: Model experiment. *J. Phys. Oceanogr.,* **25,** 2667 – 2699.

Paiva, A. M. and E. P. Chassignet, 2002: North Atlantic modeling of low frequency variability

in Mode Water Formation. *J. Phys. Oceanogr.,* **32**, 2666 – 2680.

Qiu, B, and R. X. Huang, 1995: Ventilation of the North Atlantic and North Pacific: Subduction Versus Obduction, *J. Phys. Oceanogr.,* **25**, 2374 – 2390.

Roemmich, D., S. Riser, R. Davis, and Y. Desaubies, 2004: Autonomous profiling floats: workhorse for broad scale observations. *Marine Technology Society Journal,* **38 (2)**, 21 – 29.

Talley, L. D., 1996: North Atlantic circulation and variability, reviewed for the CNLS Conference. *Physica D,* **98**, 625 – 646.

Talley, L. D., and M. E. Raymer, 1982: Eighteen degree water variability. *J. Mar. Res.,* **40 (Suppl.)**, 757 – 775.

Worthington, L. V., 1959: 18 degree water in the Sargasso Sea. *Deep-Sea Res.,* **5**, 297 – 305.

Worthington, L. V., 1977: Intensification of the Gulf Stream after the winter of 1976-77. *Nature,* **270**, 415 – 417.

Figure caption

Figure 1: (a) Number of profiles observed for each month; and (b) Float deployment locations and trajectories for all 71 floats. Dots denote the launching position.

Figure 2: Float data point distribution for (a) the worst case, January 1998, and (b) the best case, March 1999, for the period from January 1998 to December 2000. The dashed lines denote the float profiling area for the given month. (c) Outlines of the monthly float sampling domains based on all the float sampling areas from January 1998 to December 2000. Thick dashed line outlines the common domain. (d) MICOM grid points for the considered domain (dots) superimposed with float profile locations ($*$) for the best case. The dashed line represents the common domain. Solid lines along the coastlines in (a), (b), and (d) are the 200-m and 2000-m isobaths.

Figure 3: Topography in the model domain. Green solid lines are the coastlines. Red lines are the 200-m isobath used in the model. Thick solid yellow lines denote the buffer zones. The box outlined by the cyan lines defines the STMW domain.

Figure 4: Float and model temperature profiles at locations near the Panulirus Station for (a) August 1998 and (b) October 1998. Solid lines: floats; solid step-like lines: original isopycnic model profiles; dashed lines: vertically interpolated model profiles. The vertical dotted lines are 17^0C and 19^0C, respectively.

Figure 5: The mean salinity profiles at the Panulirus Station for the period from 1998 to 2000 (solid, model) and the period from 1954 to 1987 (dashed, observations after Joyce and

Robbins (1996)).

Figure 6: Meridional cross-section of model temperature at 55^0W (left panels) and at 64^0W (right panels) for winter mean (January-March) (top); summer mean (July-September) (middle), and annual mean (bottom) for years 1998 to 2000. Solid lines are model temperature profiles. Thick solid lines are model 17 and 19^0C isolines. Thick dashed lines are float 17 and 19^0C isolines.

Figure 7: Horizontal distribution of (a) float-based and (b) model-based STMW temperature, (c) float-based, and (d) model-based STMW layer thickness, (e) float-based and (f) model-based upper depth of the STMW layer, for the period 1998 - 2000.

Figure 8: Time series of (a) STMW temperature and (b) the anomalies, normalized by their standard deviation. (c) The cross-correlation between time series of float and model STMW temperature anomalies and (d) their power spectral density functions (factored by frequency). Solid lines are for floats and dashed lines are for the model. Correlations are significant at 95% level when they lie outside the dotted lines.

Figure 9: Same as Fig. 8 except for STMW volume.

Figure 10: The model annual subduction rate for the North Atlantic STMW region for (a) year 1998, (b) year 1999, (c) year 2000, and (d) the three year mean. Red lines denote the negative values and green lines denote the positive values. Thick black lines denote the zero value. Contour interval is 100 m/yr. The Panulirus Station is marked by the blue dot. The dashed lines denote the STMW formation region.

Figure 11: (a) Time evolution of model temperature profiles at the Panulirus Station for the period from January 1998 to December 2000. (b) Temperature profiles at or near the Panulirus Station for March 1998. The float profile (solid) is located at 64.2^0W, 32.2^0N and the model profile (dashed) is co-located with the Panulirus Station, which is located at 64.5^0W, 32.2^0N. The vertical dotted lines denote 17 and 19^0C, respectively.

Figure 12: (a) The time evolution of model-based annual subduction rate anomaly (integrated from an initial level formed at the end of the model spin-up run) and normalized by its standard deviation) at the Panulirus Station using both ECMWF and COADS runs. The bars represent the normalized winter NAO index anomaly. (b) The cross-correlation function between the two time series in (a). Correlations are significant at 95% level when they lie outside the dotted lines. (c) Same as (a) except that the time series is low-pass filtered with weights (1, 3, 5, 6, 5, 3, 1). The time series for low-pass filtered NAO winter index anomaly is also plotted as the dashed line. (d) The cross-correlation function between the two low-pass filtered time series in (c).

Figure 13: (a) The time evolution of low-pass filtered normalized heat flux anomaly (solid) and low-pass filtered winter NAO index anomaly (dashed line), embedded with the winter NAO index anomaly (bars) and (b) the cross-correlation function between the two time series.

Figure 14: Same as Fig. 12 except for the STMW formation region, which is defined by the area that the March mixed temperature ranges between 17^0C and 19^0C (enclosed region by the dashed lines in Fig. 10).

Figure 15: Time series of float-based STMW (a) temperature and (b) volume using different vertical temperature gradients for defining STMW. Dotted: $\frac{\partial T}{\partial z} \leq 0.006^0 C/m$ (0.006dT case); dash-dotted: $\frac{\partial T}{\partial z} \leq 0.01^0 C/m$ (0.010dT case); dash: $\frac{\partial T}{\partial z} \leq 0.25^0 C/m$ (0.025dT case); and solid: no gradient is imposed (no-dT case).

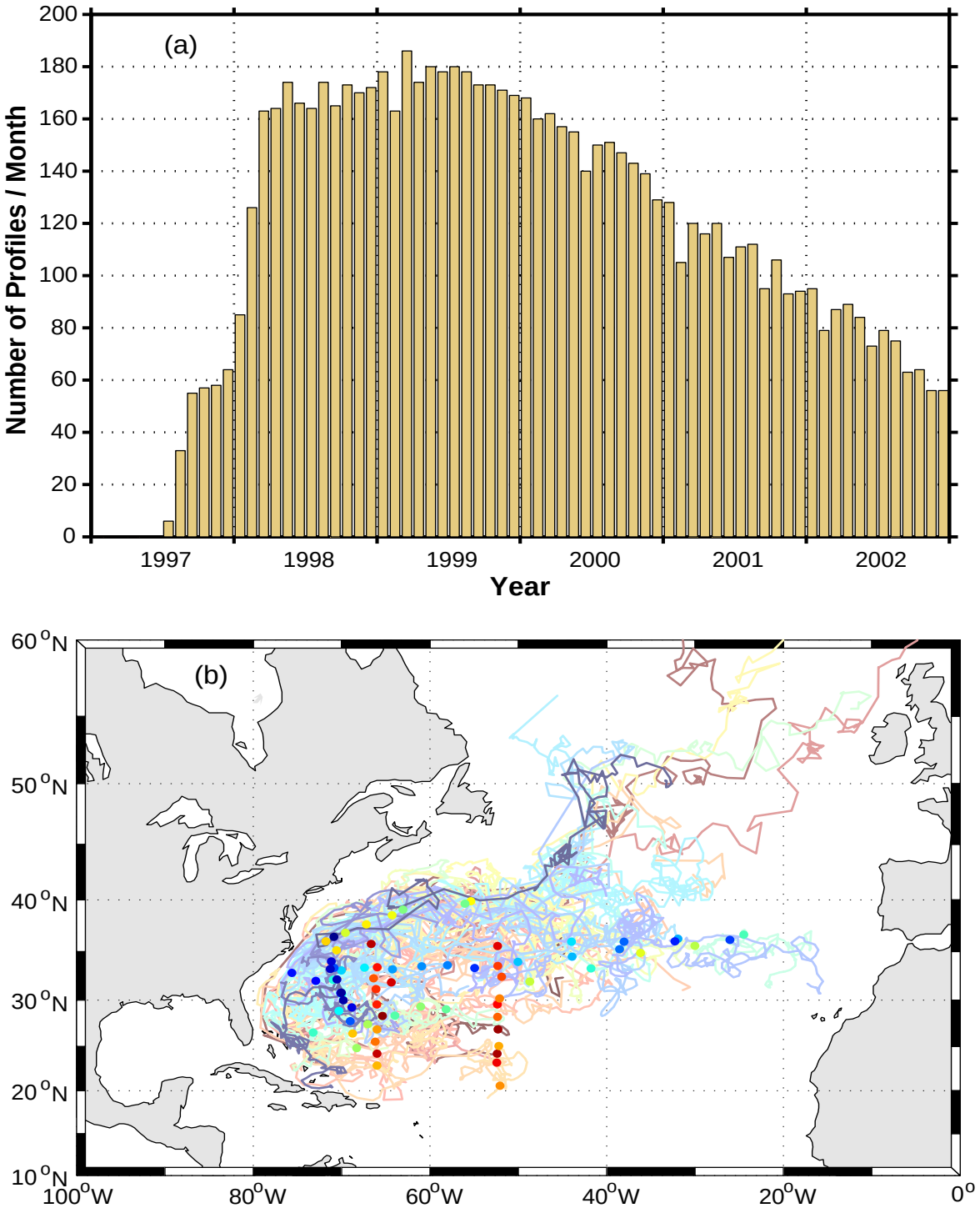

Figure 1: (a) Number of profiles observed for each month; and (b) Float deployment locations and trajectories for all 71 floats. Dots denote the launching position.

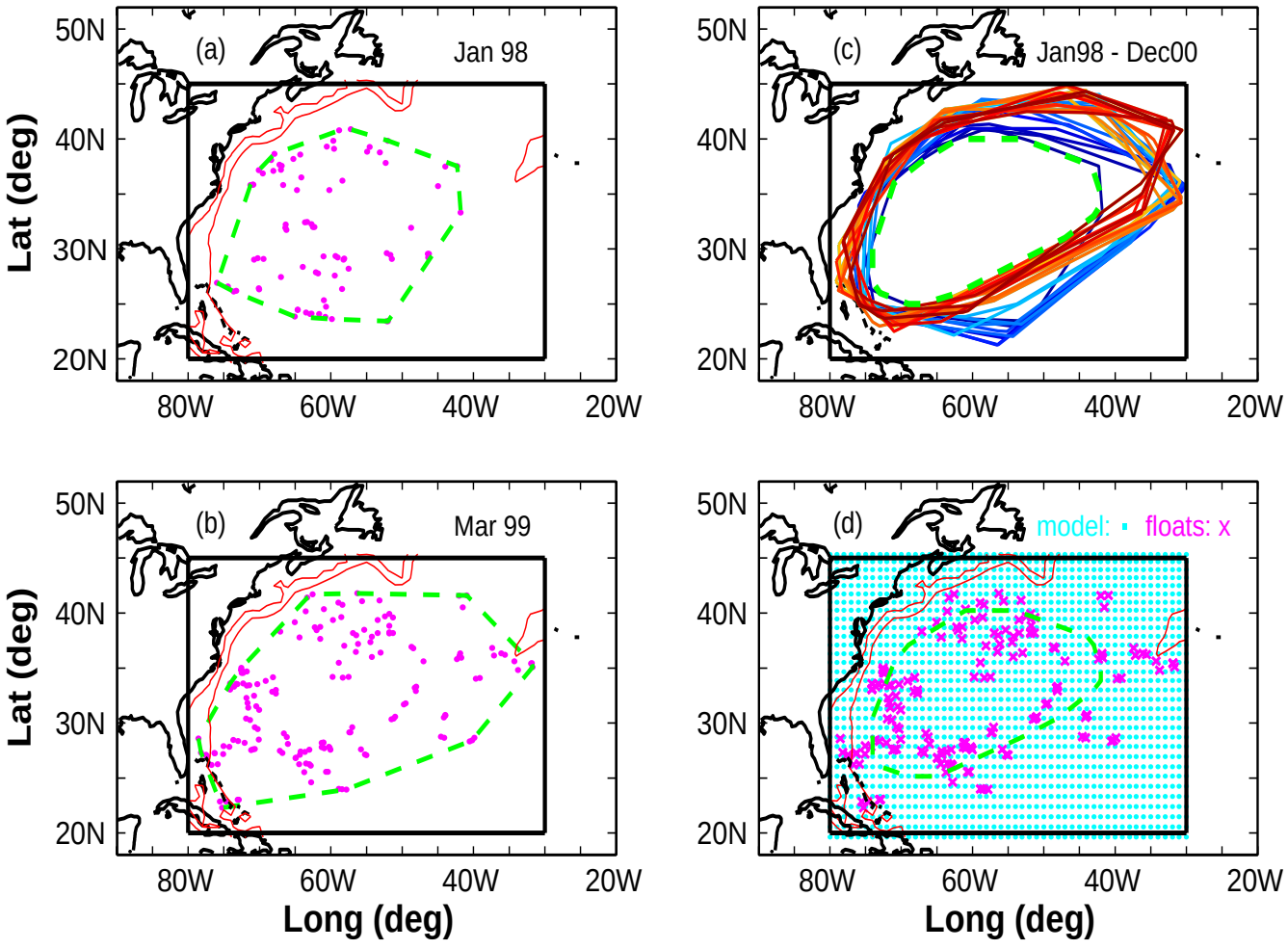

Figure 2: Float data point distribution for (a) the worst case, January 1998, and (b) the best case, March 1999, for the period from January 1998 to December 2000. The dashed lines denote the float profiling area for the given month. (c) Outlines of the monthly float sampling domains based on all the float sampling areas from January 1998 to December 2000. Thick dashed line outlines the common domain. (d) MICOM grid points for the considered domain (dots) superimposed with float profile locations ($*$) for the best case. The dashed line represents the common domain. Solid lines along the coastlines in (a), (b), and (d) are the 200-m and 2000-m isobaths.

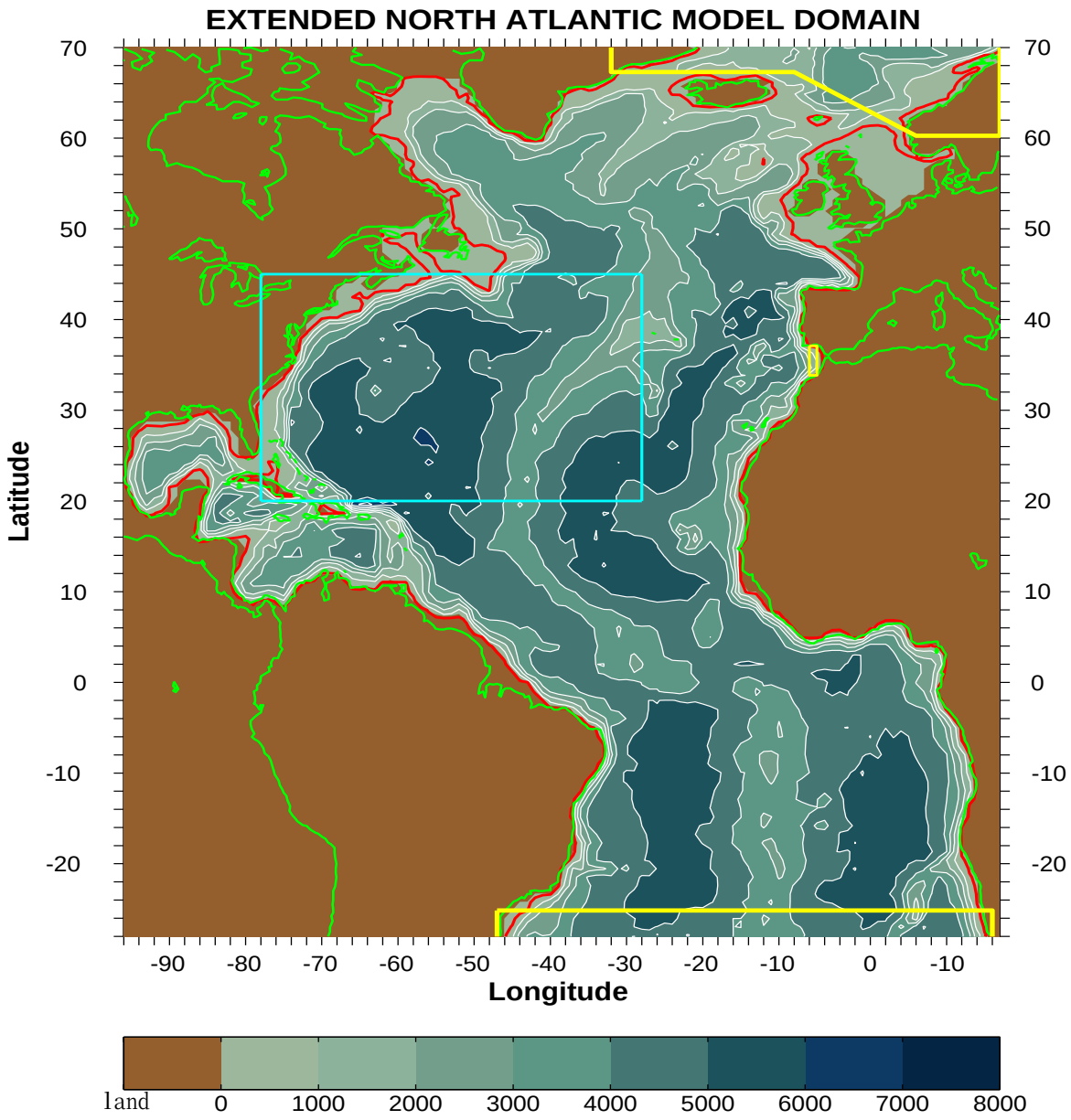

Figure 3: Topography in the model domain. Green solid lines are the coastlines. Red lines are the 200-m isobath used in the model. Thick solid yellow lines denote the buffer zones. The box outlined by cyan lines defines the STMW domain.

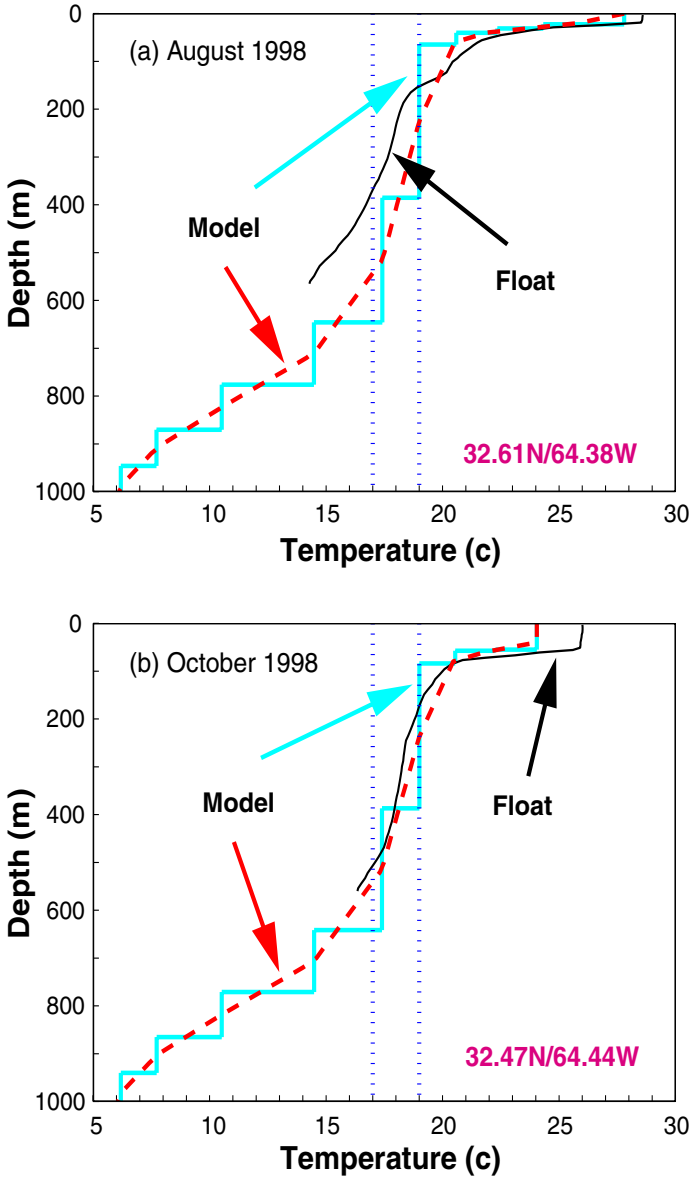

Figure 4: Float and model temperature profiles at locations near the Panulirus Station for (a) August 1998 and (b) October 1998. Solid lines: floats; solid step-like lines: original isopycnic model profiles; dashed lines: vertically interpolated model profiles. The vertical dotted lines are 17^0C and 19^0C, respectively.

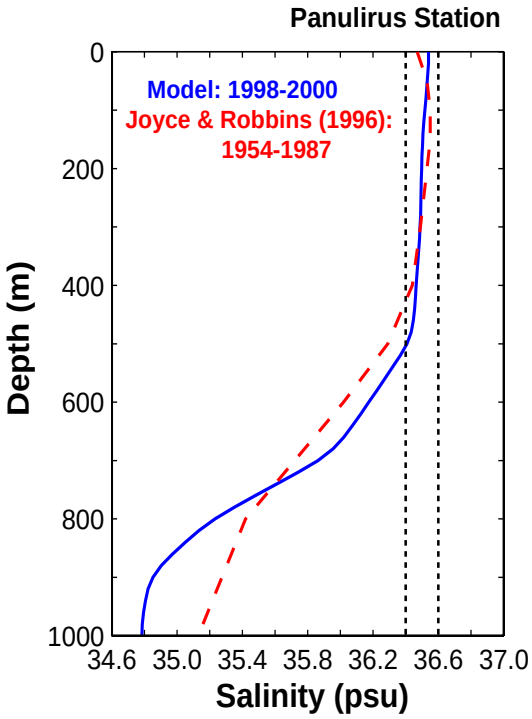

Figure 5: The mean salinity profiles at the Panulirus Station for the period from 1998 to 2000 (solid, model) and the period from 1954 to 1987 (dashed, observations after Joyce and Robbins (1996)).

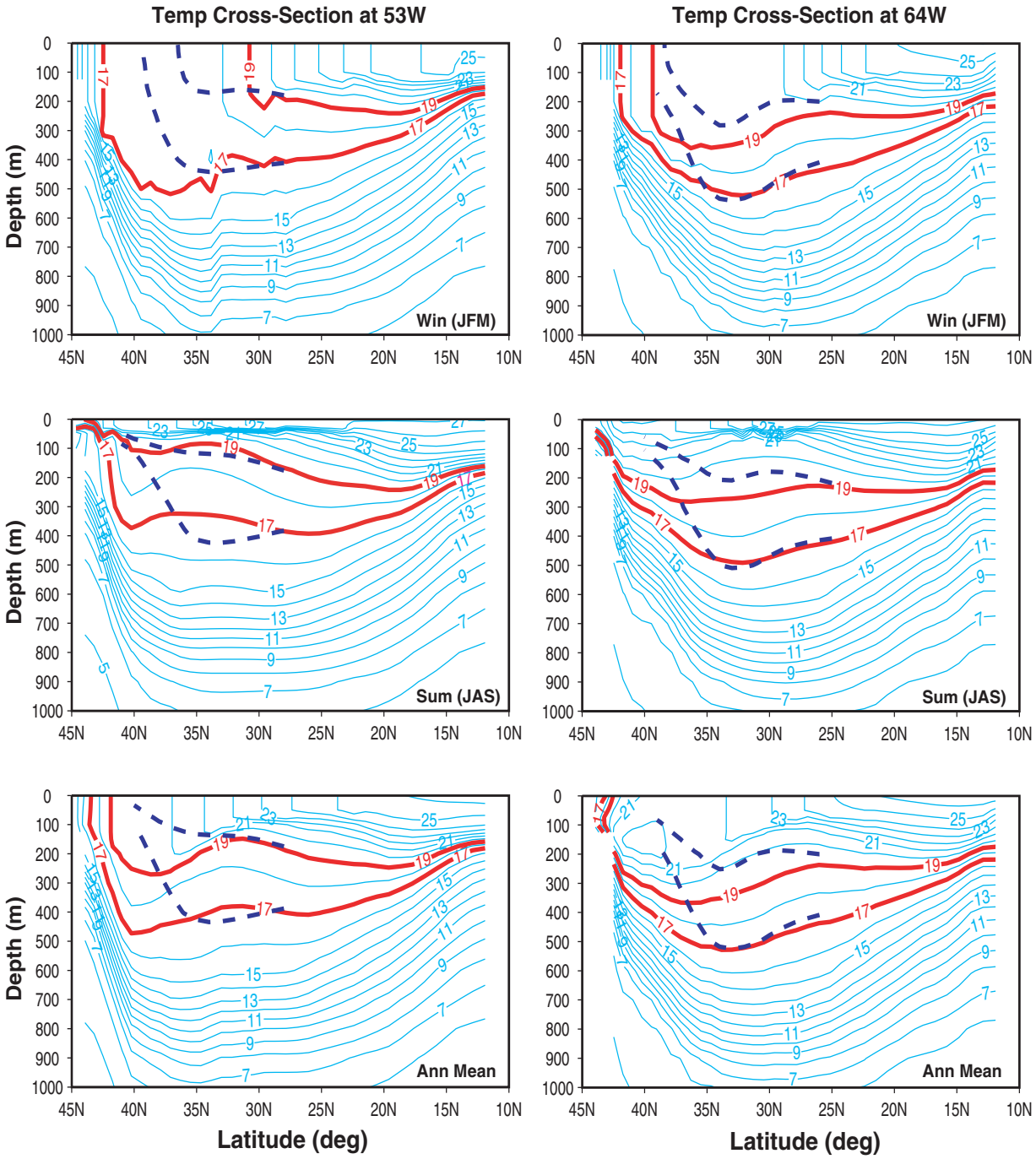

Figure 6: Meridional cross-section of model temperature at 55^0W (left panels) and at 64^0W (right panels) for winter mean (January-March) (top); summer mean (July-September) (middle), and annual mean (bottom) for years 1998 to 2000. Solid lines are for model temperature profiles. Thick solid lines are model 17 and 19^0C isolines. Thick dashed lines are float 17 and 19^0C isolines.

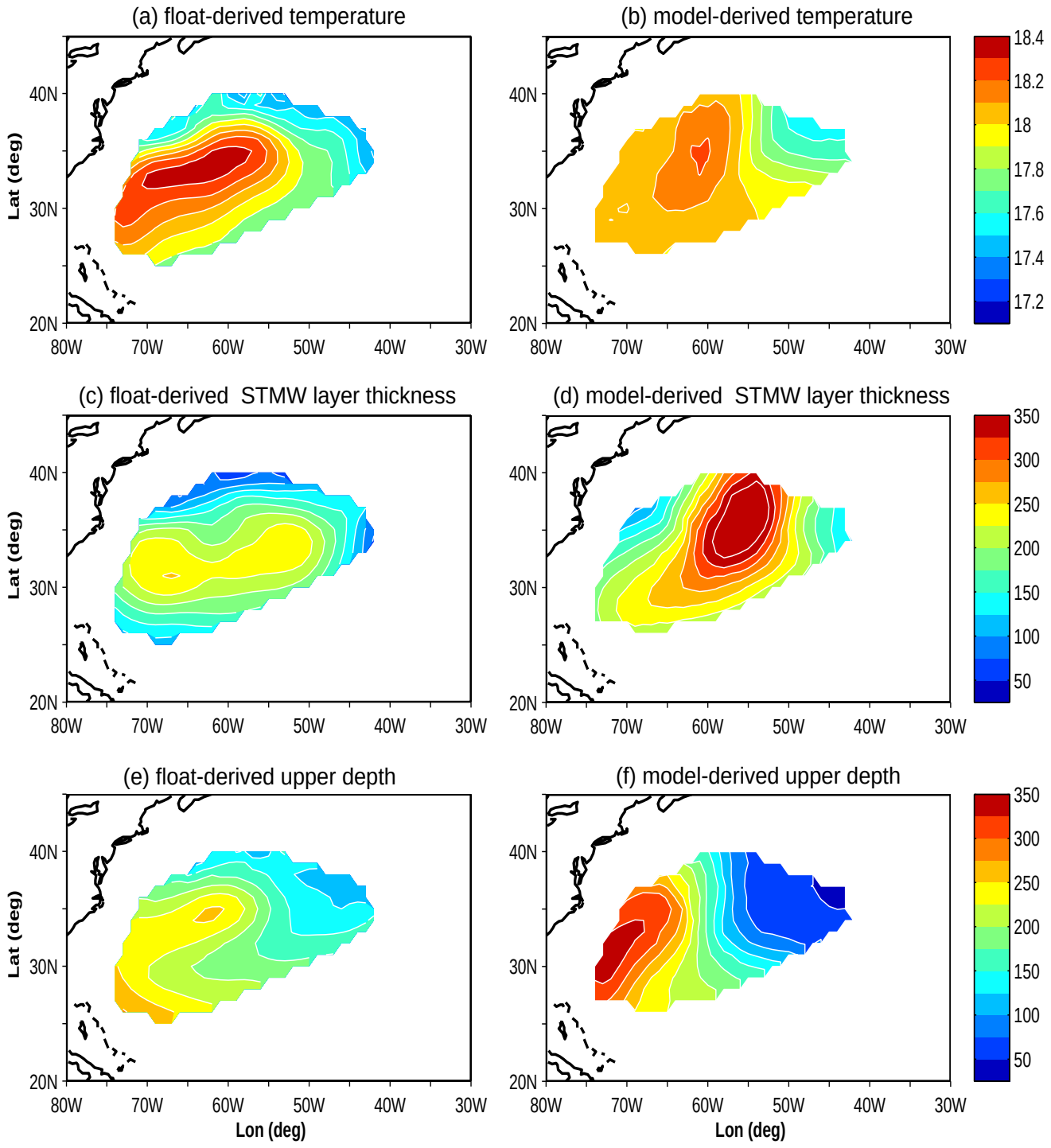

Figure 7: Horizontal distribution of (a) float-based and (b) model-based STMW temperature, (c) float-based and (d) model-based STMW layer thickness, (e) float-based and (f) model-based upper depth of the STMW layer, for the period 1998 - 2000.

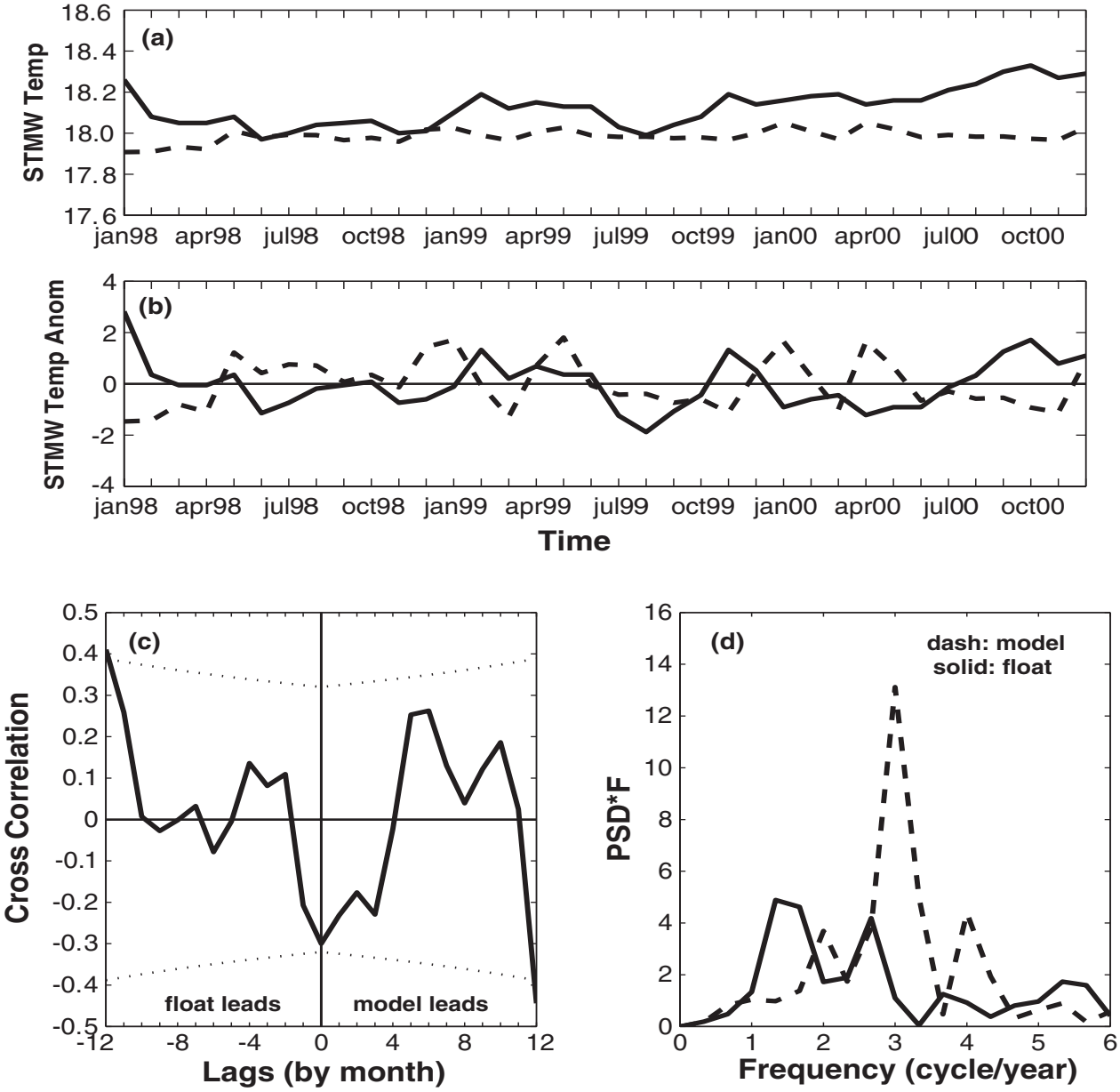

Figure 8: Time series of (a) STMW temperature and (b) the anomalies, normalized by their standard deviation. (c) The cross-correlation between time series of float and model STMW temperature anomalies and (d) their power spectral density functions (factored by frequency). Solid lines are for floats and dashed lines are for the model. Correlations are significant at 95% level when they lie outside the dotted lines.

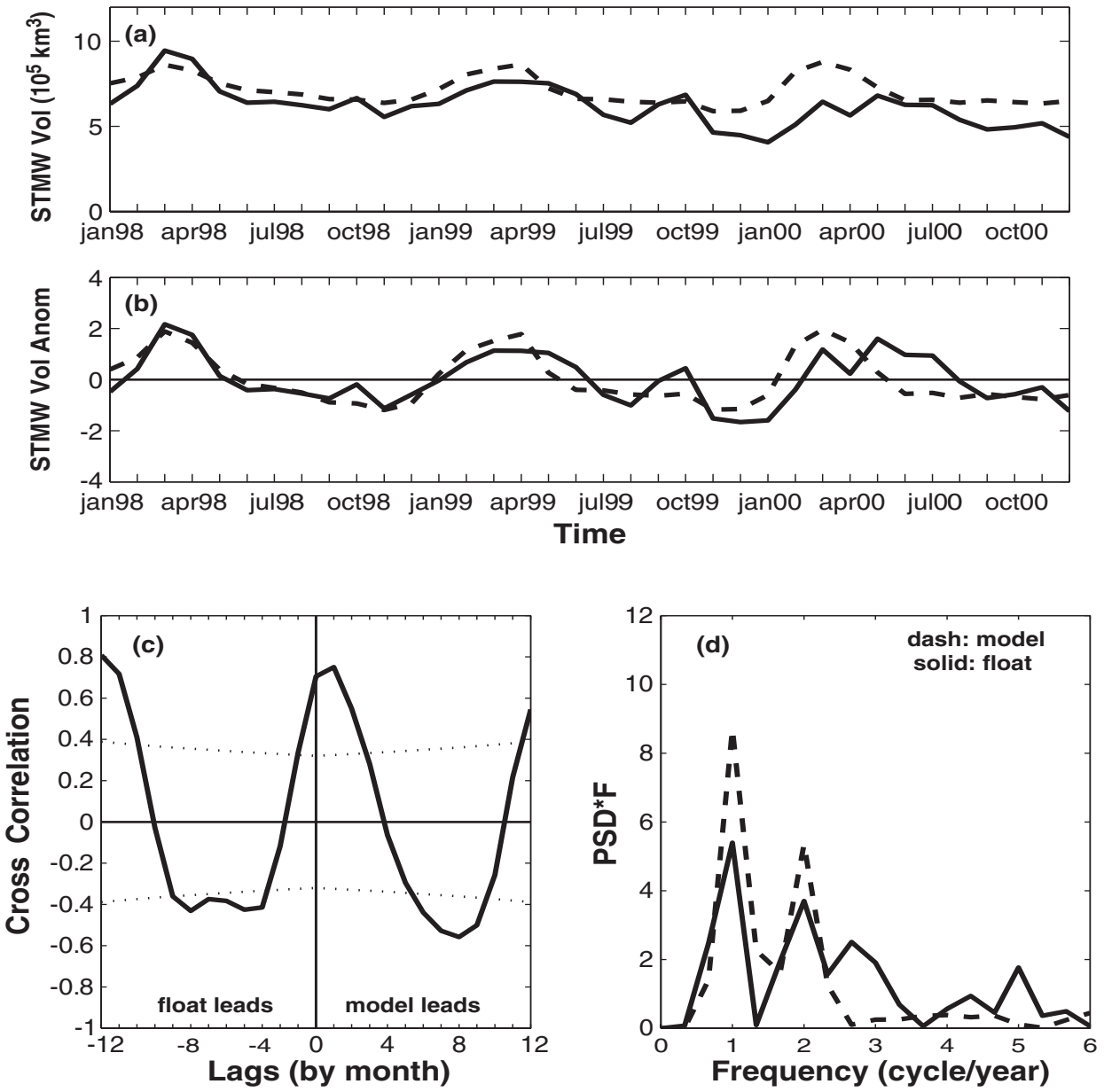

Figure 9: Same as Fig. 8 except for STMW volume.

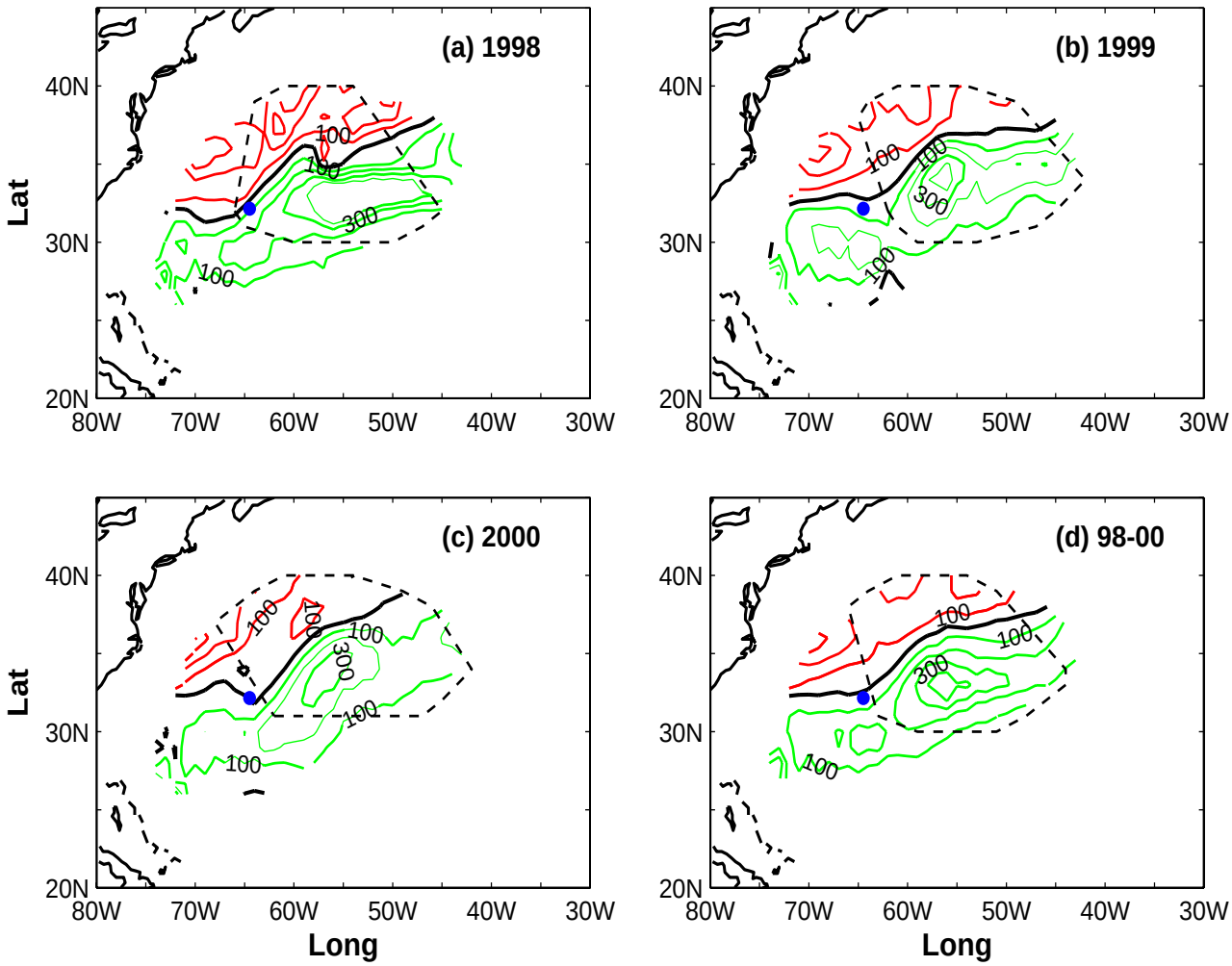

Figure 10: The model annual subduction rate for the North Atlantic STMW region for (a) year 1998, (b) year 1999, (c) year 2000 and (d) the three year mean. Red lines denote the negative values and green lines denote the positive values. Thick black lines denote the zero value. Contour interval is 100 m/yr. The Panulirus Station is marked by the blue dot. The dashed lines denote the STMW formation region.

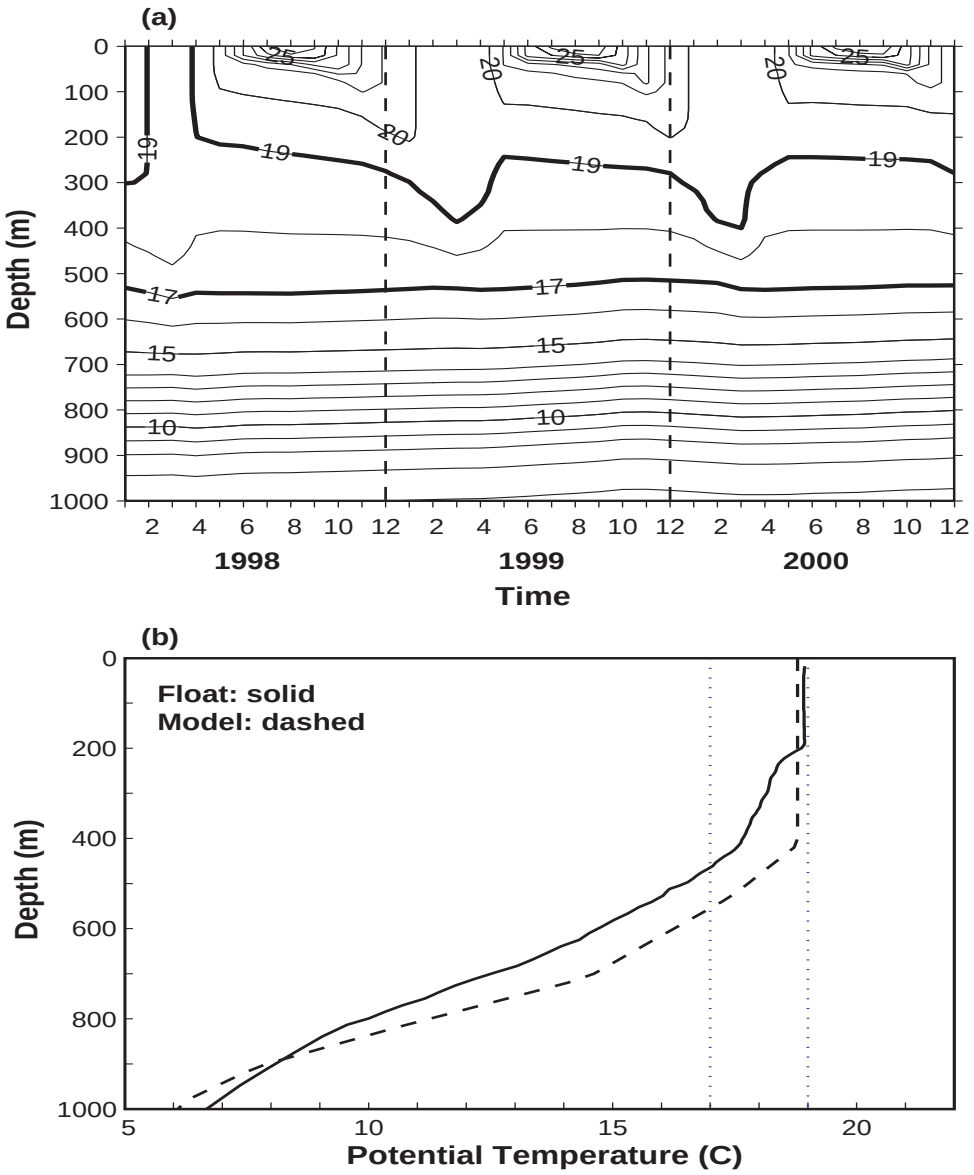

Figure 11: (a) Time evolution of model temperature profiles at the Panulirus Station for the period of from January 1998 to December 2000. (b) Temperature profiles at or near the Panulirus Station for March 1998. The float profile (solid) is located at 64.2^0W, 32.2^0N and the model profile (dashed) is co-located with the Panulirus Station, which is located at 64.5^0W, 32.2^0N. The vertical dotted lines denote 17 and 19^0C, respectively.

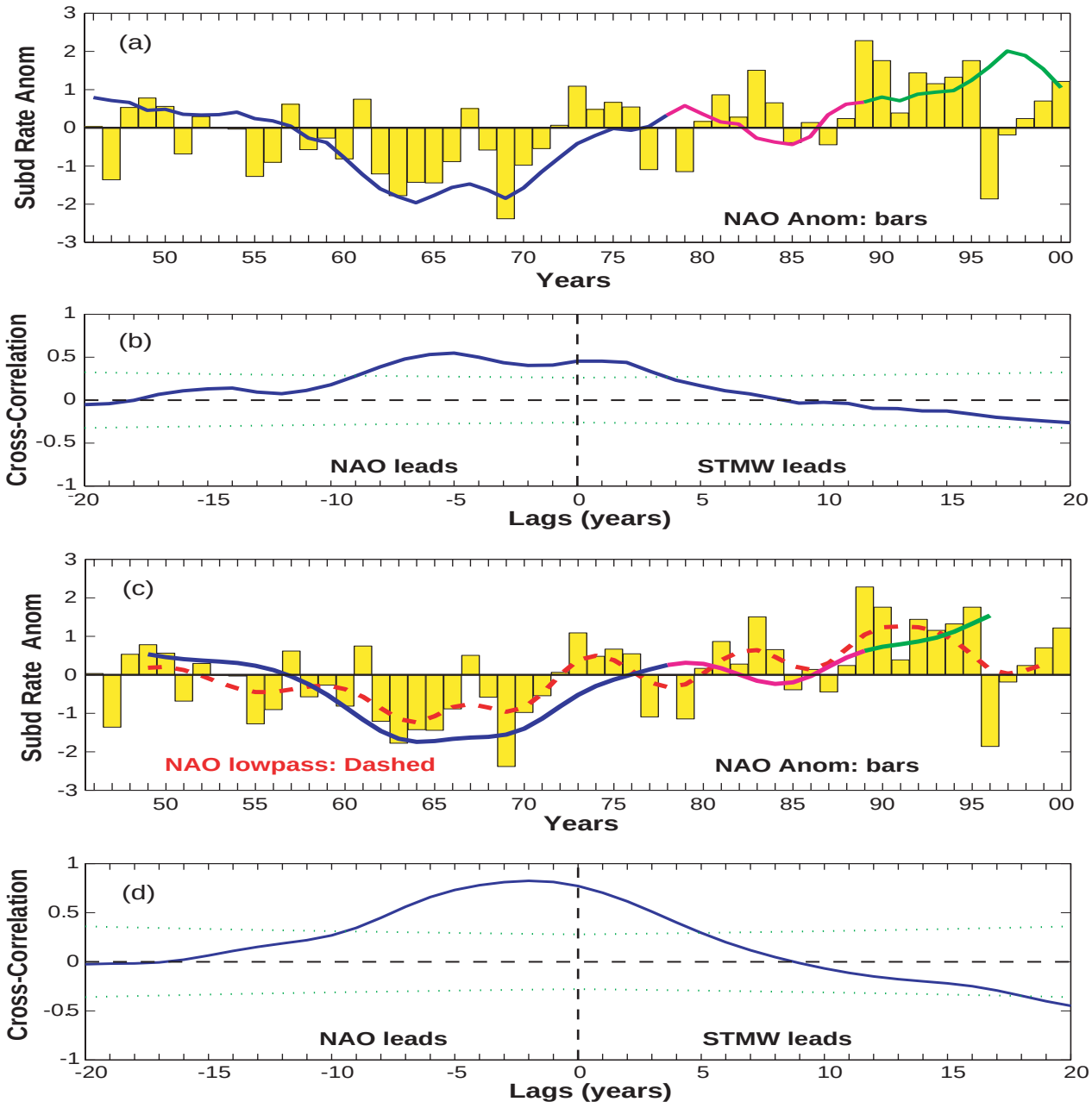

Figure 12: (a) The time evolution of model-based annual subduction rate anomaly (integrated in time and normalized by its standard deviation) at the Panulirus Station using both the ECMWF and COADS runs. The bars represent the normalized winter NAO index anomaly. (b) The cross-correlation function between the two time series in (a). Correlations are significant at 95% level when they lie outside the dotted lines. (c) Same as (a) except that the time series is low-pass filtered with weights (1, 3, 5, 6, 5, 3, 1). The time series for low-pass filtered NAO winter index anomaly is also plotted as the dashed line. (d) The cross-correlation function between the two low-pass filtered time series in (c).

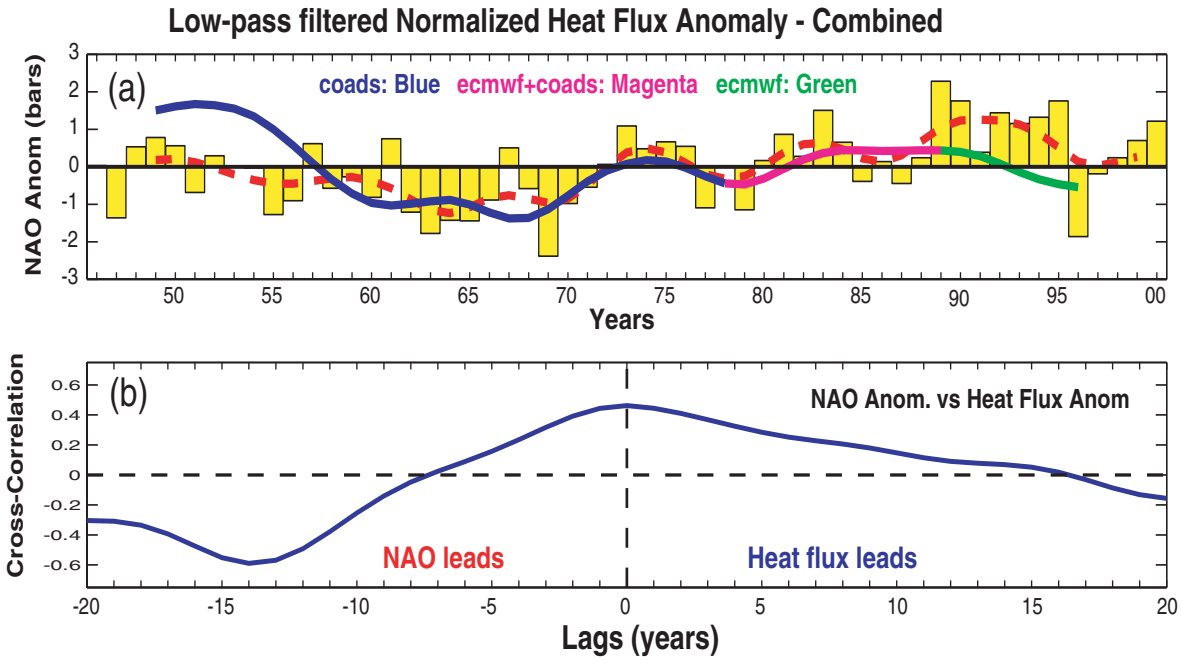

Figure 13: (a) The time evolution of low-pass filtered normalized heat flux anomaly (solid) and low-pass filtered winter NAO index anomaly (dashed line), embedded with the winter NAO index anomaly (bars), and (b) the cross-correlation function between the two time series.

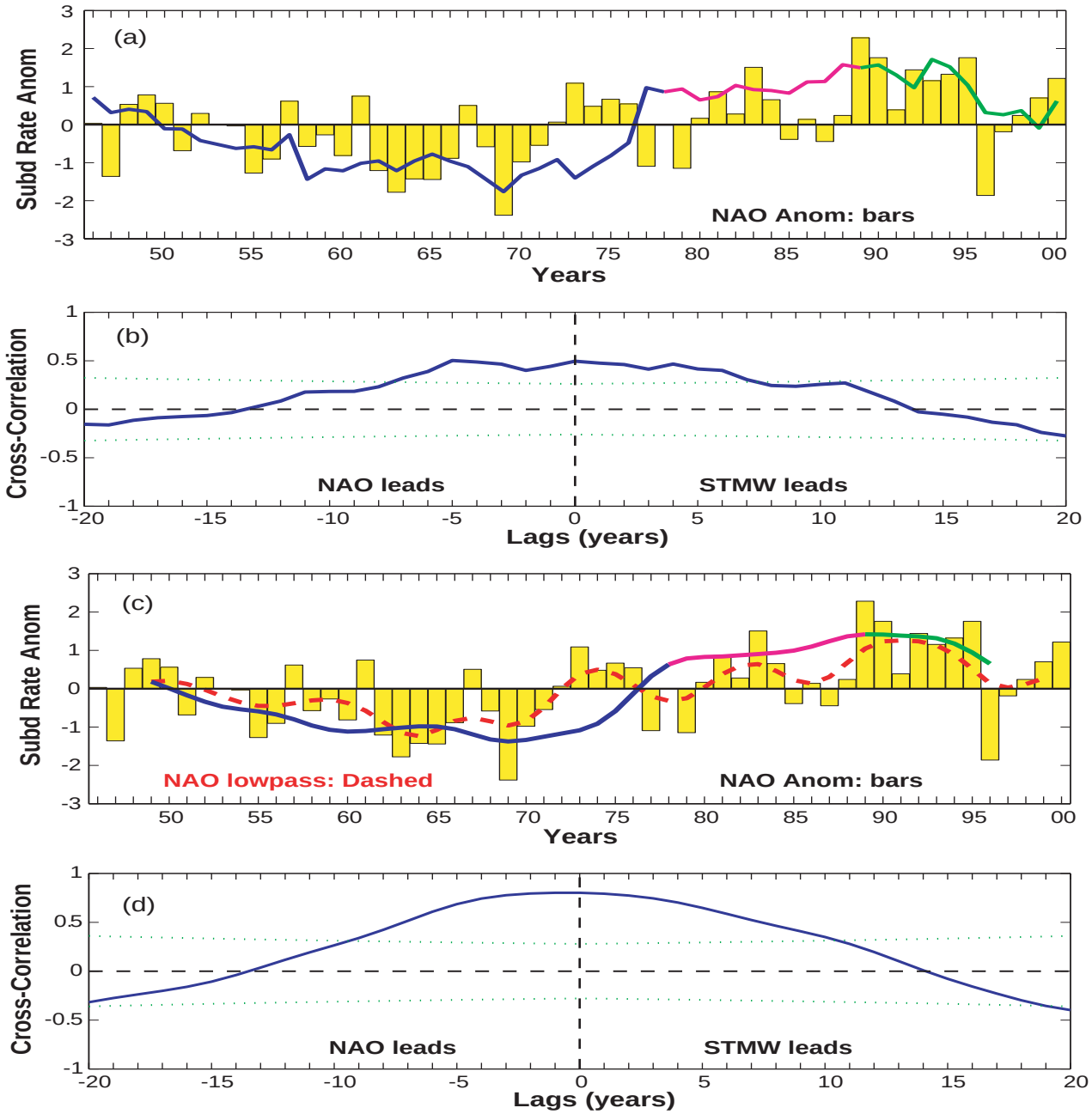

Figure 14: Same as Fig. 12 except for the STMW formation region, which is defined by the area that the March mixed temperature ranges between 17^0C and 19^0C (enclosed region by the dashed lines in Fig. 10).

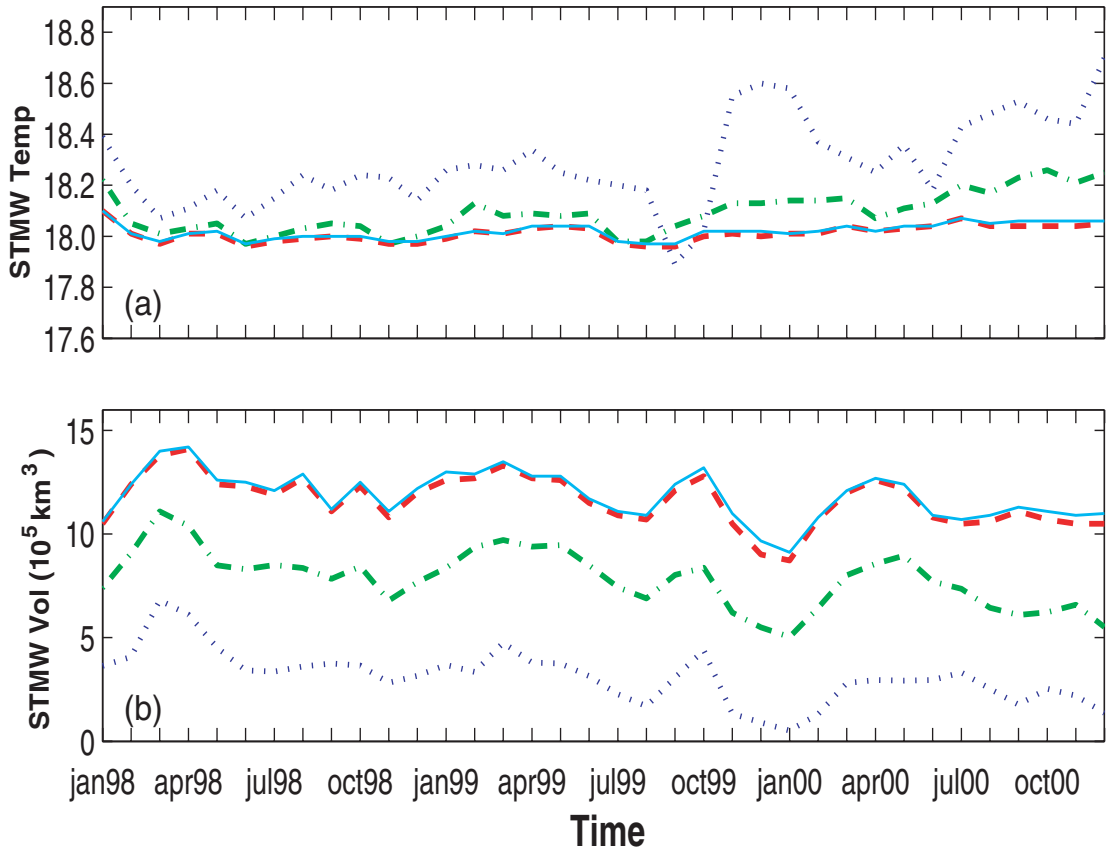

Figure 15: Time series of float-based STMW (a) temperature and (b) volume using different vertical temperature gradients for defining STMW. Dotted: $\frac{\partial T}{\partial z} \leq 0.006^0 C/m$ (0.006dT case); dash-dotted: $\frac{\partial T}{\partial z} \leq 0.01^0 C/m$ (0.010dT case); dash: $\frac{\partial T}{\partial z} \leq 0.25^0 C/m$ (0.025dT case); and solid: no gradient is imposed (no-dT case).